Atomistic Simulations of CO_2 During "Trapdoor" Adsorption onto Na-Rho Zeolite

Nathan Bamberger and Daniela Kohen

Abstract Behavior of CO_2 within Na-Rho was studied using atomistic simulations. This zeolite is known to experience a phenomenon called "cation gating" which allows carbon dioxide but not other sorbents to permeate the zeolite, giving rise to very high adsorption selectivities for CO_2. Our goal is to provide further insight into the reasons behind this intriguing phenomenon. We show that CO_2's favorable electrostatic interactions with the zeolite framework result in preferential binding in the opening of the channels between cages. This leads us to suggest a novel mechanism to explain carbon dioxide's unique "gate opening behavior" in which this preference for binding inside the "gate" allows CO_2 to "squeeze" by the gatekeeping cation as it moves around slightly due to thermal fluctuations. This proposed mechanism is distinct from a previously proposed mechanism in which carbon dioxide mediates the displacement of gatekeeping cations via electrostatic interactions and may be in better agreement with experimental evidence.

Keywords Zeolites · Cations · Trapdoor · Gating · RHO

1 Introduction

Zeolites and metal-organic frameworks are two fascinating classes of microporous adsorbents with potential applications in separation processes, catalysis, and gas storage [1–4]. In particular, these materials have received a lot of attention due to their potential ability to reduce greenhouse gas emissions through carbon-capture schemes [5, 6].

Both families of materials have advantages and disadvantages for this application, but zeolites are particularly attractive since they are already industrially synthesized, applied in large-scale processes, and can have good stability in the presence of water and other impurities. Framework structure, composition, and

---

N. Bamberger · D. Kohen (✉)
Chemistry Department, Carleton College, Northfield, MN 55057, USA
e-mail: dkohen@carleton.edu

© Springer Science+Business Media Singapore 2016

R.Q. Snurr et al. (eds.), *Foundations of Molecular Modeling and Simulation*,
Molecular Modeling and Simulation, DOI 10.1007/978-981-10-1128-3_10

location of extra-framework cations strongly influence carbon dioxide uptake in zeolites [7]. These factors also affect selectivity, which is just as important for a carbon-capture candidate as being able to strongly adsorb CO_2.

Related zeolite Rho (RHO) materials with a Si/Al framework ratio of 4.5 have shown both good CO_2 uptake and high CO_2 selectivity with respect to small molecules such as CH_4, N_2, and ethane [8–10]. As with other zeolites containing small pores connecting reasonably large cavities [11], RHO materials have window dimensions close to the kinetic diameter of the relevant gases and cage sizes that facilitate interaction with the adsorbing molecules. In addition to these characteristics, many univalent cation-exchanged zeolite Rho materials have extra-framework cations that block the entrances to the narrow pores connecting cages [9, 10]. Such materials experience a phenomenon called “cation gating” which allows carbon dioxide but not other sorbents to permeate the zeolite, giving rise to very high adsorption selectivities for CO_2. This complex behavior is a consequence of the siting and movement of these extra-framework cations but also of the strong cation-dependent structural flexibility of the Rho structure. These materials expand to accommodate carbon dioxide (and presumably no other adsorbate), but the extent of the change depends on the nature of the cation.

In this work, we focus on fully exchanged Na-Rho, the most studied Rho structure and the most promising for practical applications due to its adsorption properties and costs. Na-Rho has been extensively studied by Lozinska et al. [9, 10], who found that although it is a flexible zeolite, it retains its symmetry when loaded with 1 bar of CO_2 and distorts and expands less than other Rho materials. Lozinska et al. also performed careful in situ XRD structural studies and IR spectroscopy of carbon dioxide adsorption within this material. These studies as well as others in related Rho materials led these authors to propose a mechanism for cation gating in which cations in window sites interact strongly enough with nearby carbon dioxide molecules that the cations are temporarily displaced to empty sites within nearby α-cages, opening a “trapdoor” that allows adsorbates to diffuse through the zeolite. This intriguing mechanism is likely to be at play in other relevant materials as well. In particular, Webley and coworkers believe that a “trapdoor” mechanism is also responsible for the very high selectivity of carbon dioxide over methane that they have found in chabazite zeolites [12–14].

Because cation gating is fundamentally a molecular scale phenomenon, atomistic simulations are well-suited to help answer some of the questions left open by the experiments of Lozinska et al. due to the time-averaged nature of their data.

In this paper, we therefore present classical molecular simulations that provide detailed microscopic information regarding carbon dioxide’s “gated” adsorption within fully exchanged Na-Rho. However, the scope of this work is modest, as we only focus on the behavior of mobile cations and carbon dioxide within a rigid zeolite. This is because, to the best of our knowledge, there are no reliable atomistic potentials that can model a flexible aluminum-substituted zeolite framework. Our goal is to provide further insight into the reasons behind carbon dioxide’s ability to adsorb within cation gated zeolites rather than fully describe the system’s behavior. In particular, our results suggest that the carbon dioxide, rather than mediating the displacement of gating cations to open the trapdoor, is instead more adept than other sorbents at "squeezing" through the trapdoor as it opens by itself due to thermal fluctuations.

The remainder of the paper is structured as follows. In Sect. 2, we describe our computational methods. Section 3 presents our results and discussion: Sect. 3.1 presents cation radial distribution functions in the presence and absence of carbon dioxide, and Sect. 3.2 describes carbon dioxide and Na^+ preferred sites of adsorption. These two sections provide the rationale for the alternative scenario described in the previous paragraph and set the stage for Sect. 3.3, where we show a suggestive MD simulation of a carbon dioxide entering a "blocked" channel. We conclude in Sect. 4.

2 Methods and Models

All of our atomistic simulations were performed using standard Grand Canonical Monte Carlo (GCMC) and Equilibrium Molecular Dynamics (EMD) simulation methods. The RASPA [15] code was employed. Electrostatic energies were calculated using Ewald summation [16, 17] with a relative error of 10^{-6}. A 12 Å van der Waals cutoff was used for the short-range interactions. Periodic boundary conditions were employed.

In our GCMC simulations, four types of trial moves were used: attempts to translate an adsorbed carbon dioxide or a sodium cation, attempts to insert a new carbon dioxide into the zeolite, attempts to delete an existing carbon dioxide from the zeolite, and attempts to rotate an adsorbed carbon dioxide. Typically, simulations were run for 5×10^6 Monte Carlo cycles (each cycle consisted of max[N, 20] steps where N is the number of moving particles). The first half of these cycles was used for equilibration and was not included in the sampling of the desired thermodynamic properties. MD simulations were performed in the NVT ensemble at 298 K using a Nose–Hoover thermostat to regulate the temperature. The time step in all simulations was 0.5 fs. Each MD simulation started with a Monte Carlo (MC) pre-equilibration (at least 10^6 Monte Carlo moves) followed by MD equilibration (at least 10^6 MD steps). After equilibration, production runs of 10^6 MD steps were performed and used to sample the desired thermodynamic properties. In both, the MD and GCMC simulations, the number of steps (or cycles) was large enough that the results were independent of the number of steps.

In the work presented here, interactions between adsorbed molecules, the negatively charged zeolite framework, and extra-framework cations are modeled using a DFT-derived force field for carbon dioxide in Na-exchanged zeolites. Recently developed by Sholl's group [18] and referred to as CCFF, this potential was obtained using experimental data for zeolite LTA-4A and validated with two other common adsorbents, NaX and NaY. This makes it ideally suited for our purposes as it was designed with the goals of both being accurate and transferable to materials with the same chemical composition as Na-Rho. The CCFF potential

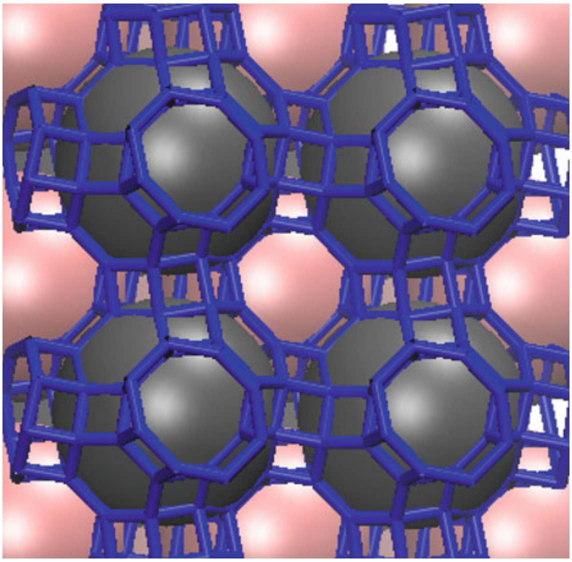

Fig. 1 The structure of zeolite Na-RHO when $P_{CO_2} = 1$ bar [20]. The framework is shown in *blue*. Note the 3-dimensional channel system composed of cavities (α-cages). Each α-cage is connected to six others by D8Rs. This gives rise to two interpenetrated but not interconnected pore systems (shown in *gray* and *pink*)

models CO_2–CO_2 interactions using the well-established EPM2 potential [19]. Within this potential, carbon dioxide is represented by a linear triatomic with fixed bond lengths and bond angles and each atom is described by a charged Lennard-Jones (LJ) center. All other interactions in the system are modeled using DFT-derived parameters. The interaction between carbon dioxide and the rest of the system has two contributions: a Coulombic and a LJ interaction between each pair of atoms. The interaction of each extra-framework cation and framework atom has a Coulombic contribution as well. In addition, the dispersion interaction between each extra-framework cation and the oxygen atoms within the framework is modeled using a Buckingham potential.

As was mentioned in the introduction, the work presented here focuses on behavior within the Na-Rho zeolite (Fig. 1). The structure of zeolite RHO is well known [20]; it has a 3-dimensional channel system composed of one size of cavities (α-cages). Each α-cage is connected to six other α-cages by double 8-ring pores (D8R). This gives rise to two interpenetrated but not interconnected pore systems. When dehydrated, zeolite Na-Rho has $I\bar{4}3m$ symmetry [9]. This zeolite is flexible: when loaded with 1 bar of carbon dioxide, the 8-rings are distorted from circular to elliptical, the α-cages become tetrahedral rather than cubic, and the zeolite expands approximately 2 % (but maintains $I\bar{4}3m$ symmetry) [10].

To the best of our knowledge, there is no available potential that would allow us to describe both the flexibility and the carbon dioxide absorption of this zeolite, and so instead, we model the system with all framework atoms fixed at their crystallographic positions while cations and carbon dioxide molecules are allowed to move. In order to make 1-to-1 comparisons regarding sites and locations within the zeolite, we wanted to use the same rigid zeolite structure for both the simulations with CO_2 and without CO_2, even though as described above the structure is known to change upon addition of CO_2. We chose to use the Na-Rho crystallographic positions corresponding to the zeolite structure when loaded with 1 bar of CO_2 [10] because our primary interest is in interactions involving CO_2. Note that most classical simulations of cation-exchanged zeolites [21, 22] also assume a rigid framework and that the CCFF potential was derived under these conditions as well. Furthermore, studies of methane in flexible LTA zeolite [23] have shown that flexibility is much less important when studying adsorption than when studying diffusion. All qualitative conclusions described in what follows were obtained using both GCMC (simulating adsorption) and MD (simulating diffusion) calculations (unless noted), lending credibility to our approach. However, the absence of a potential that can be used to more accurately study the behavior of carbon dioxide within flexible Na-Rho limits the scope of this work to the qualitative insights provided in the results and conclusion sections.

Before continuing note that when using crystallographic data obtained for Na-Rho loaded with 1 bar of CO_2, our approach is able to accurately reproduce a 298 K experimental isotherm (see Fig. 2). Note that in all the simulations presented in this work, the Si/Al ratio is approximately 4 (9.8 Al and 38.2 Si per unit cell) in order to simulate the material of interest. The positions of the Al atoms are chosen randomly subject to the constraint of Lowenstein's rule [24].

Lozinska et al. have determined that when the ratio of Si/Al $\approx$ 4, Na^+ cations preferentially occupy S8R (single 8 ring) sites and S6R (single 6 ring) sites (see Fig. 3). Our simulations of this system show cation sites that are very similar to the experimental ones in both location and fractional occupancy (see Fig. 3 and Table 1).

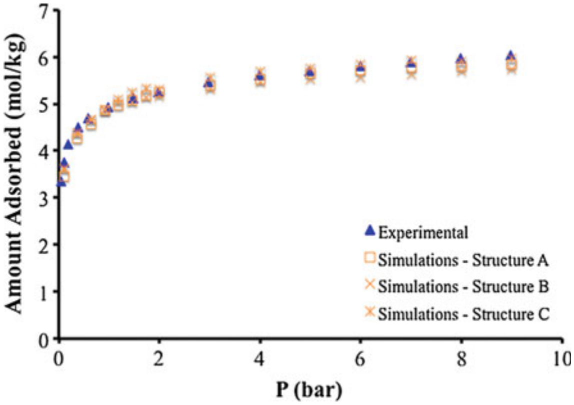

Fig. 2 CO_2 adsorption isotherm within Na-RHO at 298 K. The simulations were performed using a rigid zeolite framework with all atoms at their crystallographic positions. The three simulations shown differ in the random locations of the Al-substitutions within the zeolite. The experimental data are that of Ref. [10]

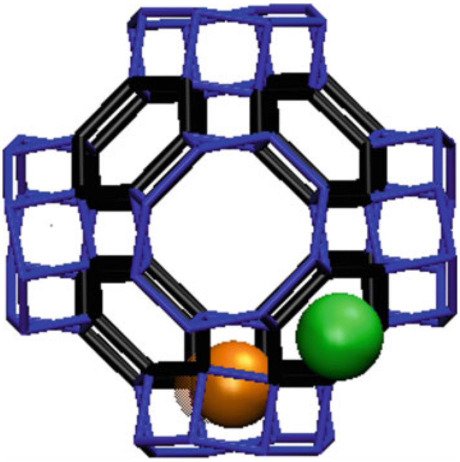

Fig. 3 Cation Sites. *Spheres* showing preferred cation sites: S8R in *orange* and S6R in *green*. The orientation of the cage was chosen to clearly show how the experimental cation site in the S8R (*solid orange sphere*) is not exactly the same as the one found in our simulations (*translucent orange sphere*); although it is not obvious in the figure, the experimental site refines in an off-center position. Note that the experimental S6R site is indistinguishable from the one found in this work. The figure also shows the D8R traced in *blue* and the S6R traced in *black*. Note that in each unit cell, there are 6 D8R sites (and thus 12 S8R) and 8 S6R. The experimental data are that of Ref. [10]

Table 1 Fractional occupancies of cation sites

Sample (P_{CO_2})		Occ. fraction site S8R	Occ. fraction site S6R
Na-RHO (0 bar)	Experimental	0.51	0.43
	Simulations	0.48	0.41
Na-RHO (1 bar)	Experimental	0.5	0.49
	Simulations	0.46	0.40

Experimental data are from Ref. [10]. Note that in our calculations, as in experiments, about half the S8R are blocked by cations whether carbon dioxide is present or not. Lozinska et al. argue that it is likely that cations prefer to occupy S8Rs belonging to different D8Rs. However, our calculations show that is not the case. This could be another shortcoming of the interaction potentials we are using, but without further evidence, this cannot be ascertained

3 Results and Discussion

3.1 Cation Radial Distribution Function

The equilibrium positions of cations in the presence and absence of carbon dioxide were first investigated by calculating radial density probability functions. Figure 4 shows the average of 5 such plots from different GCMC runs where the random Al

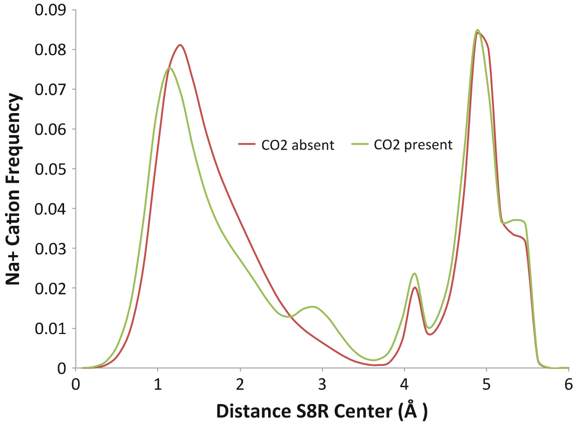

Fig. 4 Cation radial probability density functions. Each line is the average of 5 plots from different GCMC runs where the random Al locations were all the same but the seed numbers were different. Note that the distributions do not differ substantially between when carbon dioxide is present and when it is not. In both cases, there is a peak near zero corresponding to the S8R site and another much further away corresponding to cations on the S6R site. However, while the distribution of cations in the S6R is essentially unchanged, there is a small shift in the distribution of cations in the S8R when carbon dioxide is present: The probability of a cation being between 1–2 Å from the center of the ring is smaller while around 3 Å the probability is larger than in the absence of the adsorbate

locations were all the same, but the seed numbers were different. Note that the qualitative conclusions reached below can be obtained by examining each of these five runs independently or equivalent MD runs, but averaging allows the reader to focus on the important features. Also note that the conclusions are the same if the random Al-substitutions are different. The zero was chosen as the crystallographic center of an S8R. This position was chosen because a cation sitting near the center of the S8R blocks carbon dioxide molecules from also fitting in the plane of the ring. Figure 4 shows that the distributions do not vary much between when carbon dioxide is present and when it is not. In both cases, there is a peak near zero (corresponding to the cations in the S8R site) and another peak 4–6 Å away corresponding to cations in the S6R site. However, there is one difference that is important in the context of this article: While the distribution of cations in the S6R does not change appreciably, there is a shift in the distribution of cations in the S8R when carbon dioxide is present. More specifically, when CO_2 is added to the zeolite the probability of a cation being located 1–2 Å from the center of the ring decreases while at around 3 Å the probability increases. In other words, there is a net movement of some cations away from the center of the 8 rings when CO_2 is introduced into the zeolite, a finding that is in agreement with the experimental observation that CO_2 is not blocked by cations. However, this finding does not address the issue of what causes some cations to move from their blocking positions and allow for the “opening of the gate.” We therefore move on to this question in the following sections.

3.2 Preferred Sites of Adsorption

In this section, preferred sites of adsorption for both carbon dioxide and cations will be investigated. These will suggest that the reason for carbon dioxide's "gate opening behavior" has more to do with carbon dioxide's preferred sites within the zeolite than its ability to guide cations out of the way.

Figures 5 and 6 show probability maps for sodium cations and carbon dioxide molecules, respectively, at 298 K. These maps are normalized 3D histograms of particle locations collected every 10 cycles during a GCMC simulation with 5×10^6 production cycles. Qualitatively equivalent results are obtained if data are collected in an EMD simulation. The maps in Fig. 5 correspond to cation locations when no carbon dioxide is present, but almost identical ones are obtained in the presence of 1 bar of CO_2. This demonstrates that only limited cation rearrangement takes place when carbon dioxide is adsorbed, just as experiments have suggested [9]. In Fig. 5a, the scale is such that even locations that are very infrequently visited are shown. This map reveals that cations explore within their site and thus must somehow be mobile. The extent to which this mobility is poor is underscored in Fig. 5b, where only the region within the 0.1*max probability contour is shown.

Figure 6 shows that, as expected, the carbon dioxide molecules explore a large region of the zeolite; the figure highlights the cages and the narrow passages between then. This plot suggests that the highest probability of finding an adsorbed CO_2 is at the entrances of the narrow channels connecting cages (i.e., in the S8R). This finding is in line with previous work within silica-only zeolites ITQ-3 and ZK4 (an LTA equivalent) [25, 26] where we have shown that carbon dioxide, but not nitrogen, strongly adsorbs in narrow pores between cages. Carbon dioxide adsorption in the narrow pores takes on increased significance in the context of this paper because to enter these pores the CO_2 must pass the cation that is "gating" the S8R.

Figure 7a shows that carbon dioxide has two preferred adsorption sites: one in the S8R, as mentioned previously, and the other, near the walls of the α-cage. These locations are in agreement with findings by Lozinska and coworkers [10] who were also able to locate carbon dioxide molecules in two sites, one within the window region and another within the cage. Figure 7 was obtained by using appropriate symmetry operations to collapse probability anywhere in the simulation cell around a location at the geometric center of the D8R. This effectively moves all the probability around any of the D8Rs in the simulation cell to the vicinity of the one shown, highlighting the role of this region. Figure 7b is an equivalent plot for the sodium cations. Figure 7 shows how both cations and carbon dioxide have a preferred site of adsorption near the center of the S8R.

In their work, Lozinska et al. suggest that blocking cations undergo a quick CO_2-mediated migration from a window site to an empty S6R site, "opening the gate" for a brief period of time and allowing CO_2 to diffuse through. They suggest that weaker electrostatic interactions between cations and other adsorbents prevent this mechanism from taking place with molecules such as CH_4. The plots in Fig. 7 suggest an alternative explanation for carbon dioxide's ability to permeate the

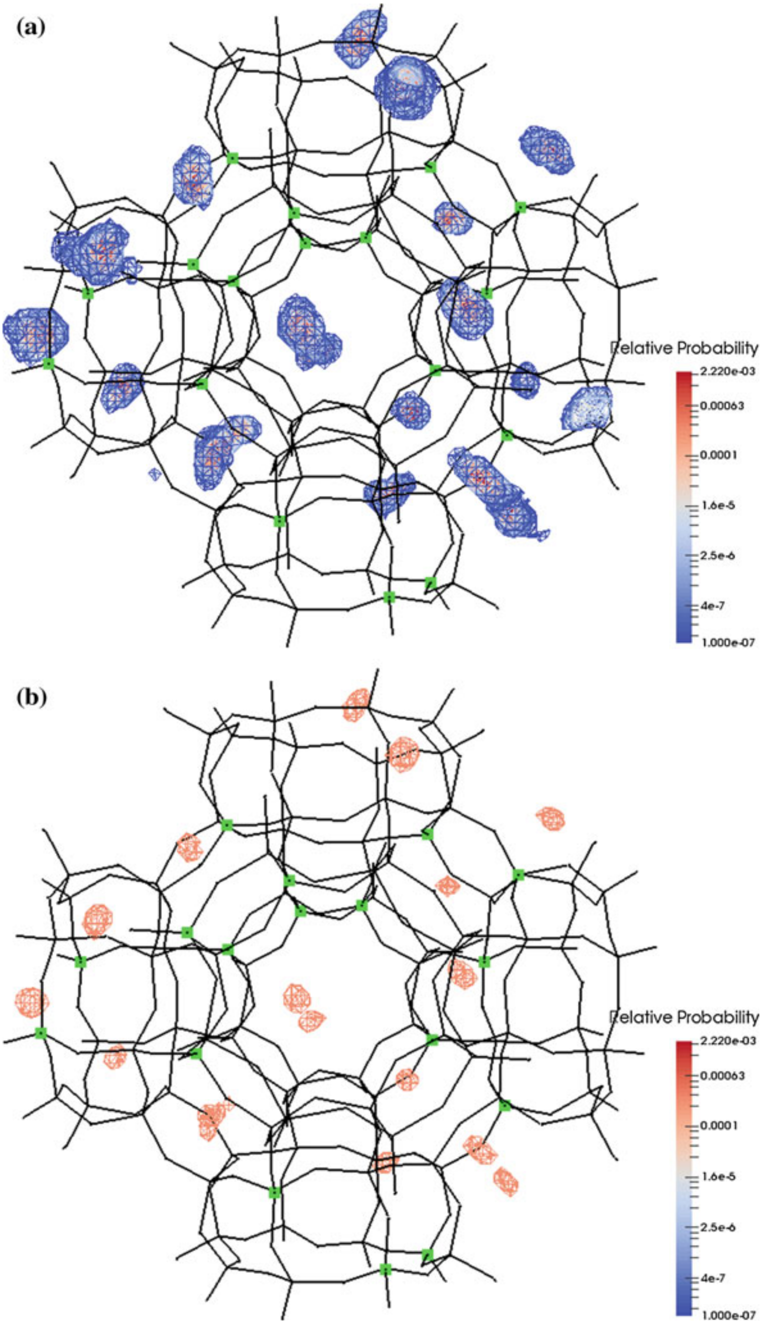
(a)
Relative Probability
2.220e-03
0.00063
0.0001
1.6e-5
2.5e-6
4e-7
1.000e-07
(b)
Relative Probability
2.220e-03
0.00063
0.0001
1.6e-5
2.5e-6
4e-7
1.000e-07

◀ **Fig. 5** Probability map for sodium cations. The figure is centered in the middle of a cage, with six D8Rs surrounding it. The framework is shown in *black* with the Al atoms in *green*. **a** The probability scale is such that even locations that are very infrequently visited are shown in *blue*. These *blue* regions reveal that the cations explore within their site and are thus to some extent mobile. **b** Most visited locations (the 0.1*max probability contour is shown)

zeolite: perhaps the gating cation periodically moves around the S8R by itself due to thermal motion, and CO_2 is simply more inclined than other molecules to "squeeze" by into the S8R when this happens due to its natural affinity for this site. In other words, it is not so much that the carbon dioxide molecule opens the gate by interacting with the "gatekeeper" sodium, but rather that carbon dioxide is able to take advantage of a "wandering gatekeeper." In the context of this alternative explanation, Fig. 4 can be understood as showing the cation distribution changing due to competition with the CO_2 for the ring site.

Within this alternative explanation, a methane molecule, for example, would not be able to take advantage of the cation's thermal motion because in the absence of strong electrostatic interactions with the pore it might lack carbon dioxide's preference for an S8R site. At this moment, there is no methane potential that would allow us to further confirm this hypothesis, but to explore the plausibility of this explanation we ran simulations in which we artificially set CO_2's partial charges to

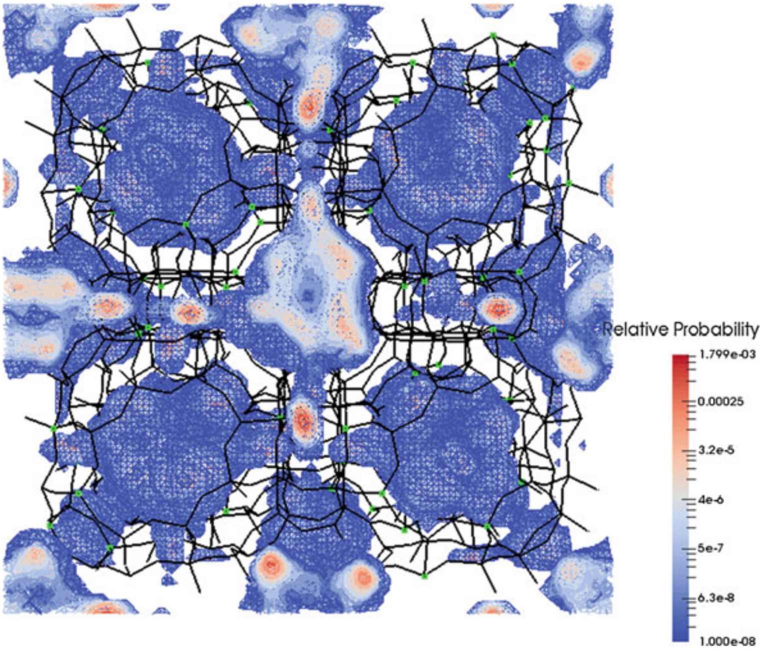

Fig. 6 Probability map for carbon dioxide. The figure shows a 2 × 2 × 2 simulation cell. The framework is shown in *black* with the Al atoms in *green*. The figure highlights the cages and the narrow passages in between then

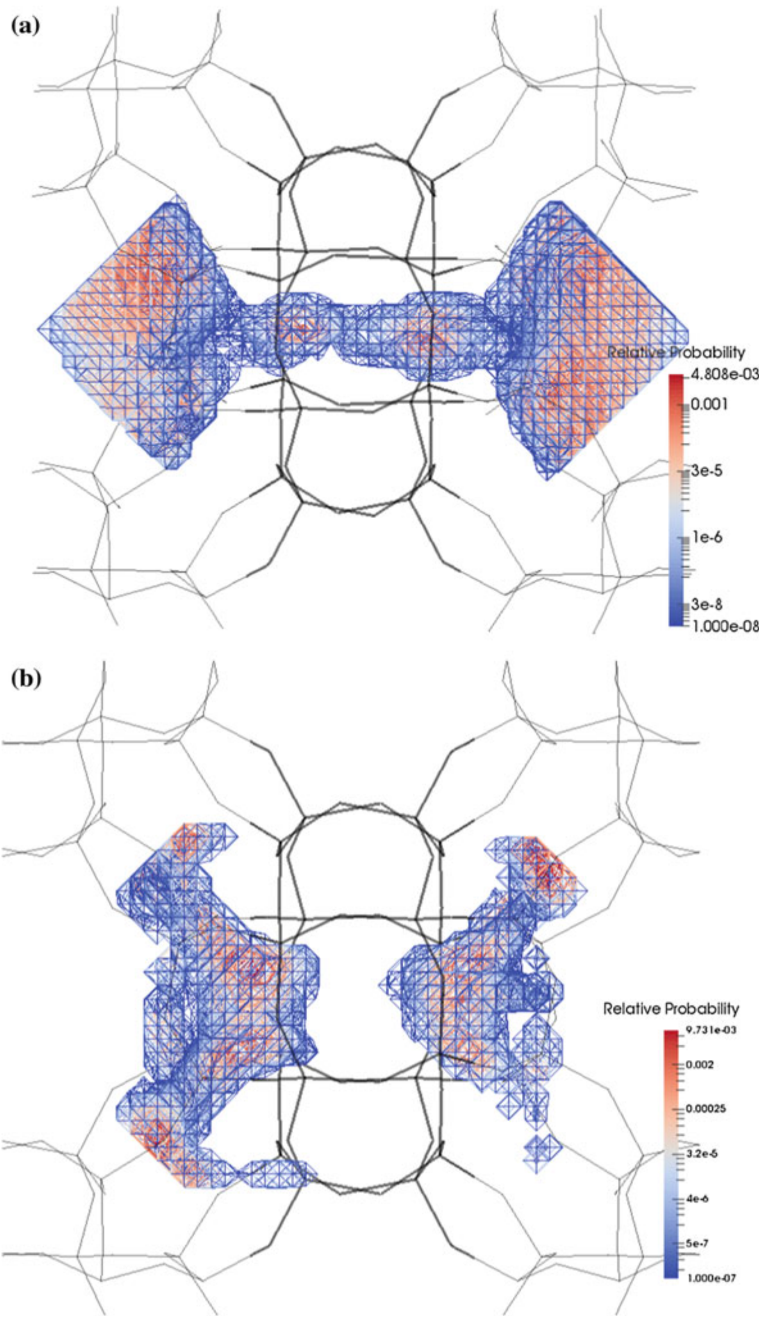
(a)
Relative Probability
4.808e-03
0.001
3e-5
1e-6
3e-8
1.000e-08
(b)
Relative Probability
9.731e-03
0.002
0.00025
3.2e-5
4e-6
5e-7
1.000e-07

◀ **Fig. 7** Probability maps around a D8R. *Thicker lines* highlight the D8R. These plots were obtained by using appropriate symmetry operations to collapse probability anywhere in the simulation cell around a location at the geometric center of the D8R. This effectively collapses all the probability around any of the D8Rs in the simulation cell to the vicinity of the one shown, highlighting the role of this region. **a** Map for carbon dioxide. Note the areas of higher probability in the middle of each S8R and near the walls of the α-cage. The map does not include CO_2 probability corresponding to empty D8R sites. **b** Map for sodium cations. Note the areas of higher probability at the sites mentioned, in the S8R and in the S6R

zero. In previous work within silica-only zeolite [25, 27], we have used this strategy to show that when carbon dioxide is modeled using only dispersive forces, it no longer strongly adsorbs in the narrow pores between cages and this region becomes a barrier to diffusion rather than an adsorption site. Under these conditions, carbon dioxide's preferred sites become quite similar to those of nitrogen (the other adsorbent studied in those articles). Figure 8 is the equivalent of Fig. 7a for when carbon dioxide's partial charges are set to zero. Note how in this case the middle of each S8R is no longer a preferred location. This suggests that a molecule without a significant quadrupole would not "squeeze" into the S8R, and thus, its diffusion would be blocked by the cation in the S8R. This might explain why other small molecules are not able to diffuse within this material [8–10] while carbon dioxide is.

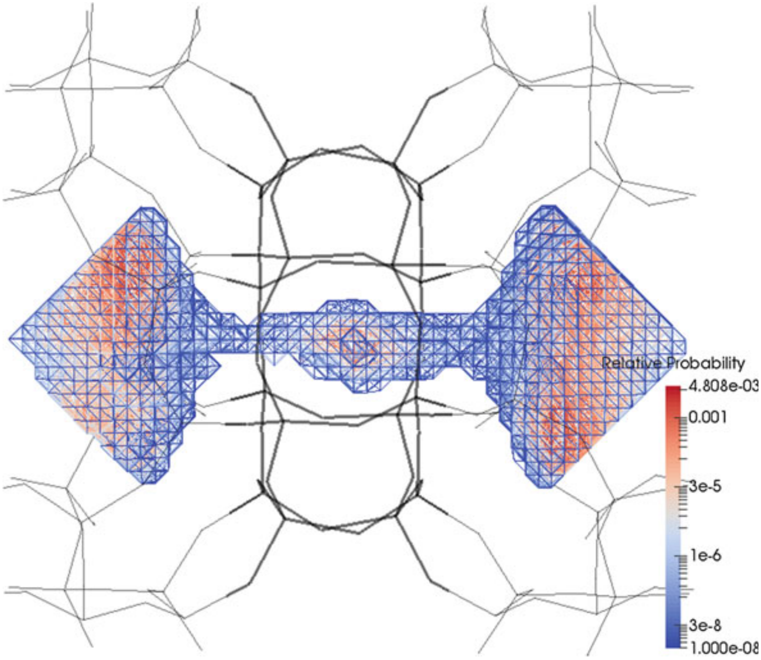

Fig. 8 Carbon dioxide probability maps around a D8R when CO_2's partial charges are set to zero. The map does not include CO_2 probability corresponding to empty D8R sites. Note how the areas of higher probability differ from those in Fig. 7a in that the middle of each S8R is no longer a preferred location

3.3 An MD Trajectory Showing a CO_2 Entering a "Gated" Ring

A carbon dioxide entering a cation-blocked narrow channel between two α-cages (the D8R) is likely a rare event. Given the importance of such an event in the context of this work, many MD simulations were searched in order to find one. Figure 9 shows a carbon dioxide molecule entering a D8R that is blocked by a cation. Figure 9a is a snapshot, Fig. 9b traces the motion of the carbon dioxide, and Fig. 9c traces the cation (a 0.5-ns movie showing this event is available as supplemental information). This figure shows how little the cation moves as the carbon dioxide

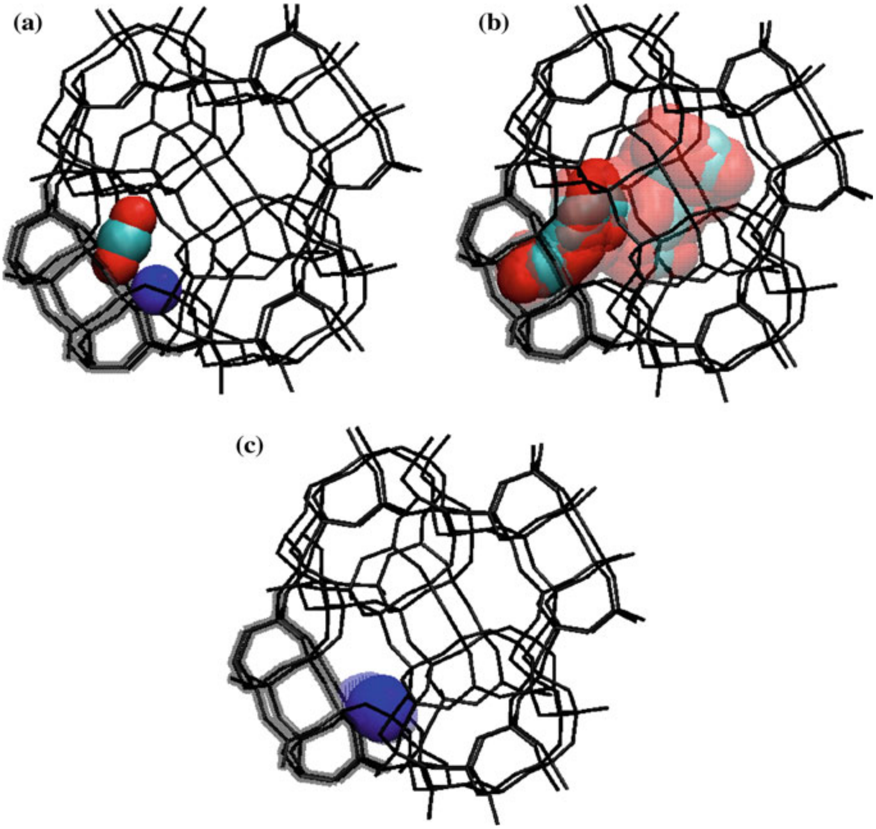

Fig. 9 A carbon dioxide molecule entering a D8R blocked by a cation. Only the relevant adsorbate molecule and cation are shown in the figure. The blocked D8R is highlighted. **a** A snapshot. **b** Multiple frames showing the motion of the CO_2. *Solid colors* show 0.5 ps before and after the frame shown in (**a**) while translucent shows 50 ps before and after. **c** Multiple frames showing the very narrow range of motion of the blocking cation. Frames 0.5 ps before and after the frame in (**a**) are shown in *solid blue*, frames 50 ps before and after are shown in *blue stripes*, and frames 200 ps before and after are shown as translucent *blue*

enters the ring, and in particular that while our simulations show that when the cation and carbon dioxide are close to each other electrostatic interactions cause them to interact strongly, we have found no evidence that the cation needs to leave the S8R site in order to allow for a carbon dioxide molecule to enter the "gate." This finding is significant in the context of CO_2/CH_4 breakthrough experiments performed by Palomino et al. [8] on zeolite Na-RHO. These experiments showed that while CO_2 is retained, methane passes with practically no retention. If the cation truly does leave the narrow channel via a CO_2-facilitated jump from a S8R site to a S6R site (as in the mechanism suggested by Lozinska et al.), even for a short time, then molecules other than carbon dioxide might be able to pass through the gate. On the other hand, a cation that only moves slightly away from the S8R could completely block methane from entering the zeolite. Our proposed mechanism may therefore be in better agreement with the Palomino results than that of Lozinska et al.

It is important to point out, though, that our mechanism and Lozinska's are not mutually exclusive: It is entirely possible that CO_2 being better at opening the gate and CO_2 being better at entering the gate when it opens by itself (due to thermal fluctuations) both contribute to carbon dioxide's ability to diffuse through the zeolite while other molecules cannot.

4 Conclusions

We have used molecular simulations to examine the behavior of CO_2 within Na-Rho zeolite focusing on the manner by which pore blocking sodium cations allow this adsorbate to diffuse within the material. Experiments have shown that while carbon dioxide can explore this zeolite (and other related zeolites), other small gas molecules such as nitrogen and methane cannot, effectively making Na-RHO zeolite a very attractive candidate for practical separations. While this highly selective trapdoor adsorption is thought to be a consequence of both the cation behavior and the framework flexibility, we focus in this work only on the former. Despite this shortcoming, our work identifies a novel understanding of the mechanism at play: rather than coaxing the cation off the blocking position by interacting via electrostatic forces, a carbon dioxide competes with the cation for the position at the entrance of the channel and so is able to squeeze by as the cation moves around its adsorption site (the whole system is at room T). We show that carbon dioxide has a preferred site at the S8R, which disappears when electrostatic forces are artificially ignored. This suggest that gases that do not possess a quadrupole cannot diffuse through S8Rs because they have no energetic reason for entering the narrow channel when then the cation is not quite blocking the S8R.

Our work highlights the need for reliable atomistic potentials for other cations and other adsorbates that would allow this mechanism to be studied further. Potentials that would allow for a flexible zeolite are also needed. We believe the potential used here is adequate to shed light onto the behavior, but its inability to describe motion of the framework is a significant shortcoming. Experimentally it has been shown that carbon dioxide but not other gases can penetrate and thereby distort the zeolite. Our work suggests carbon dioxide’s preference for the S8R might influence (and even drive) this geometry change, but the available potentials do not allow us to investigate this hypothesis further. Further improvements in the available force fields would allow for better understanding of materials with doorkeeping cations and their interactions with adsorbates with and without a quadrupole and thus aid the search for microporous materials uniquely suited to practical CO_2 separations.

Acknowledgments N.B. and D.K. gratefully acknowledge the Petroleum Research Fund (PRF# 51765-UR5) and National Science Foundation (CHE-1039925) for computing resources and stipend support to carryout this research.

References

1. Choi, S., Drese, J.H., Jones, C.W.: Adsorbent materials for carbon dioxide capture from large anthropogenic point sources. Chemsuschem **2**, 796–854 (2009)
2. Keskin, S., Sholl, D.S.: Efficient methods for screening of metal organic framework membranes for gas separations using atomically detailed models. Langmuir **25**, 11786–11795 (2009)
3. Yazaydin, A.O., Snurr, R.Q., Park, T.H., Koh, K., Liu, J., LeVan, M.D., Benin, A.I., Jakubczak, P., Lanuza, M., Galloway, D.B., Low, J.J., Willis, R.R.: Screening of metal-organic frameworks for carbon dioxide capture from flue gas using a combined experimental and modeling approach. J. Am. Chem. Soc. **131**, 18198–18199 (2009)
4. Di Biase, E., Sarkisov, L.: Systematic development of predictive molecular models of high surface area activated carbons for adsorption applications. Carbon **64**, 262–280 (2013)
5. D’alessandro, D.M., Smit, B., Long, J.R.: Carbon dioxide capture: prospects for new materials. Angew. Chem. Int. Edit. **49**, 6058–82 (2010)
6. Pera-Titus, M.: Porous inorganic membranes for CO_2 capture: present and prospects. Chem. Rev. **114**, 1413–1492 (2014)
7. Grajciar, L., Cejka, J., Zukal, A., Arean, C.O., Palomino, G.T., Nachtigall, P.: Controlling the adsorption enthalpy of CO_2 in zeolites by framework topology and composition. Chemsuschem **5**, 2011–2022 (2012)
8. Palomino, M., Corma, A., Jorda, J.L., Rey, F., Valencia, S.: Zeolite Rho: a highly selective adsorbent for CO_2/CH_4 separation induced by a structural phase modification. Chem. Commun. **48**, 215–217 (2012)
9. Lozinska, M.M., Mangano, E., Mowat, J.P.S., Shepherd, A.M., Howe, R.F., Thompson, S.P., Parker, J.E., Brandani, S., Wright, P.A.: Understanding carbon dioxide adsorption on univalent cation forms of the flexible zeolite rho at conditions relevant to carbon capture from flue gases. J. Am. Chem. Soc. **134**, 17628–17642 (2012)
10. Lozinska, M.M., Mowat, J.P.S., Wright, P.A., Thompson, S.P., Jorda, J.L., Palomino, M., Valencia, S., Rey, F.: Cation gating and relocation during the highly selective “trapdoor” adsorption of CO_2 on univalent cation forms of zeolite rho. Chem. Mater. **26**, 2052–2061 (2014)
11. Cheung, O., Hedin, N.: Zeolites and related sorbents with narrow pores for CO_2 separation from flue gas. RSC Adv. **4**, 14480–14494 (2014)
12. De Baerdemaeker, T., De Vos, D.: Gas separation trapdoors in zeolites. Nat. Chem. **5**, 89–90 (2013)

13. Shang, J., Li, G., Singh, R., Gu, Q.F., Nairn, K.M., Bastow, T.J., Medhekar, N., Doherty, C. M., Hill, A.J., Liu, J.Z., Webley, P.A.: Discriminative separation of gases by a "molecular trapdoor" mechanism in chabazite zeolites. J. Am. Chem. Soc. **134**, 19246–19253 (2012)
14. Shang, J., Li, G., Singh, R., Xiao, P., Liu, J.Z., Webley, P.A.: Determination of composition range for "molecular trapdoor" effect in chabazite zeolite. J. Phys. Chem. C **117**, 12841–12847 (2013)
15. Dubbeldam, D., Calero, S., Ellis, D.E., Snurr, R.Q.: RASPA: molecular simulation software for adsorption and diffusion in flexible nanoporous materials. Mol. Simul. (2015)
16. Allen, M.P., Tildesley, D.J.: Computer Simulations of Liquids. Oxford Science Publications (1994)
17. Frenkel, D., Smit, B.: Understanding Molecular Simulation: From Algorithms to Applications. Academic Press, London (1996)
18. Fang, H.J., Kamakoti, P., Ravikovitch, P.I., Aronson, M., Paur, C., Sholl, D.S.: First principles derived, transferable force fields for CO_2 adsorption in Na-exchanged cationic zeolites. Phys. Chem. Chem. Phys. **15**, 12882–12894 (2013)
19. Harris, J.G., Yung, K.H.: Carbon dioxides liquid-vapor coexistence curve and critical properties as predicted by a simple molecular-model. J. Phys. Chem.-Us. **99**, 12021–4 (1995)
20. Robson, H.E., Shoemake, D.P., Ogilvie, R.A., Manor, P.C.: Synthesis and crystal-structure of zeolite rho—new zeolite related to linde type-A. Adv. Chem. Ser. 106–15 (1973)
21. Calero, S., Dubbeldam, D., Krishna, R., Smit, B., Vlugt, T.J.H., Denayer, J.F.M., Martens, J. A., Maesen, T.L.M.: Understanding the role of sodium during adsorption: a force field for alkanes in sodium-exchanged faujasites. J. Am. Chem. Soc. **126**, 11377–11386 (2004)
22. Garcia-Sanchez, A., Ania, C.O., Parra, J.B., Dubbeldam, D., Vlugt, T.J.H., Krishna, R., Calero, S.: Transferable force field for carbon dioxide adsorption in zeolites. J. Phys. Chem. C **113**, 8814–8820 (2009)
23. Garcia-Sanchez, A., Dubbeldam, D., Calero, S.: Modeling adsorption and self-diffusion of methane in LTA zeolites: the influence of framework flexibility. J. Phys. Chem. C **114**, 15068–15074 (2010)
24. Loewenstein, W.: The distribution of aluminum in the tetrahedra of silicates and aluminates. Am. Mineral. **39**, 92–96 (1954)
25. Madison, L., Heitzer, H., Russell, C., Kohen, D.: Atomistic simulations of CO_2 and N_2 within cage-type silica zeolites. Langmuir **27**, 1954–1963 (2011)
26. Selassie, D., Davis, D., Dahlin, J., Feise, E., Haman, G., Sholl, D.S., Kohen, D.: Atomistic simulations of CO_2 and N_2 diffusion in silica zeolites: the impact of pore size and shape. J. Phy. Chem. C **112**, 16521–16531 (2008)
27. Goj, A., Sholl, D.S., Akten, E.D., Kohen, D.: Atomistic simulations of CO_2 and N_2 adsorption in silica zeolites. The impact of pore size and shape. J. Phys. Chem. B **106**, 8367–8375 (2002)